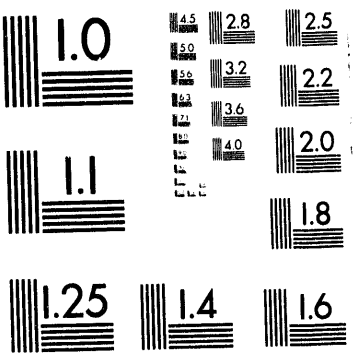
1.0
1.1
1.25
1.4
1.6
1.8
2.0
2.2
2.5
2.8
3.2
3.6
4.0
4.5
5.0
5.6
6.3
7.1
8.0

1 of 1

Conf-931133--8

UCRL-JC-114136
PREPRINT

Resonant Photoemission and Magnetic X-Ray Circular Dichroism in the M Shell of Ultrathin Films of Fe

J. G. Tobin
G. D. Waddill

This paper was prepared for submittal to
Journal of Applied Physics
MMM Conference
Minneapolis, MN
November 15-19, 1993

September 27, 1993

Lawrence Livermore National Laboratory

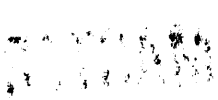

RESONANT PHOTOEMISSION AND MAGNETIC X-RAY CIRCULAR DICHROISM IN THE M SHELL OF ULTRATHIN FILMS OF FE

J.G. Tobin and G.D. Waddill

Lawrence Livermore National Laboratory

Chemistry and Materials Science Department

Livermore, CA 94550 • USA

ABSTRACT

Using magnetic ultrathin films (2–4 ml) of Fe on Cu(001) and bulk-like Fe, the Fe3p and Fe3s core states have been investigated with resonant photoemission and core-level photoemission, including magnetic x-ray circular dichroism (MXCD) experiments. The resonant photoemission experiment has been done in fine steps over a wide photon energy range ($h\nu$ = 695eV–715eV), to probe the parentage of various spectral structures. The onset of secondary channels at the L_3($h\nu$ = 707eV) and L_2($h\nu$ = 720eV) edges will be analyzed in light of results from bulk Ni (Reference 1). The MXCD photoelectron spectroscopy of the Fe3p exhibits a 0.2eV shift with circular polarization variation. The previously observed split peak structure in the Fe3s (Reference 2) will be discussed with regard to the new resonant photoemission results. The resonant photoemission results will also be put into the context of our MXCD absorption results for monolayer (Reference 3) and multilayers (Reference 4) of Fe.

INTRODUCTION

Although the observation of spin-dependent splitting in photoelectron spectroscopy of magnetic materials has become fairly common, a complete understanding of the causes remains elusive. For example, consider the case of the M shell core levels of Fe. The Fe3s exhibits a doublet peak

structure that can be observed with non-helically polarized x-rays and without a spin detector[2] or separated by use of spin-sensitive detection[5,6]. The Fe3p has been shown to have a splitting with circular polarization[7], spin-detection[8,9], and even with linear polarization in a spin integrated mode (linear dichroism)[10]. Examples of these splittings are shown in Figures 1, 2, and 3: In Figure 1, an Fe3p in 2 ML of Fe/Cu(001); in Figure 2 (top-most spectrum) the Fe3s of 4 monolayer (ML) of Fe/Cu(001) displays a split peak; and in Figure 3 (top-most spectrum), a bulk-like Fe sample [25 ML of Fe on Cu(001)] also exhibits an asymmetrically-split Fe3s peak. The lower spectra in Figures 2 and 3 are examples of resonant photoemission[11], where additional channels for electron emission have opened up as the $2p_{3/2}$ and $2p_{1/2}$ core-level thresholds were reached (Figure 4). The interplay of the direct and resonance channels is a means to test theories concerning the origin of the 3s peak splitting, as discussed in Reference 1. Here, we will present detailed resonant photoemission spectra of Fe/Cu(001) and bulk-like Fe which will call into question the analysis advocated in Reference 1.

EXPERIMENTAL

These experiments were performed at the Stanford Synchrotron Radiation Laboratory, using the University of California/National Laboratories Participating Research Team facilities, on the spherical grating monochromator (SGM) beamline[12], Beamline 8–2. Both Beamline 8–2 (Reference 13) and Beamline 8–1 (Reference 14), a torroidal grating monochromator, have been demonstrated to be very high resolution instrumentation. Beamline 8–2 can also be used as a source of circularly-polarized x-rays[2–4,7]. The data was collected in a three-tiered, two-chamber photoelectron spectrometer[15], equipped for photoemission with full energy and angular (±3°) resolution and multi-channel detection.

DISCUSSION

In resonant photoemission, new channels open up with the crossing of each core-level threshold. In Figures 2 and 3, major spectral changes occur at hν = 707eV ($2p_{3/2}$ threshold) and hν = 720eV ($2p_{1/2}$ threshold). Because of finite energy broadening, the onset of these changes often occur at photon energies just below the nominal threshold. New spectral features can be seen at the valence bands ($B^F \equiv 0$; B^F is the binding energy with respect to the Fermi energy), the Fe3p (B^F = 53eV) and the Fe3s (B^F = 92eV). As the photon energies are increased, the new features move across the spectra, with a constant kinetic energy (KE) associated with each feature. A summary of constant BF and constant KE features is shown in Table 1. In fact, these constant KE features can be viewed as Auger peaks. In the third column of Table 1 are values taken from an Auger handbook[17]: All except one are printed-assigned values, with the exception being 620eV, which corresponds to a smaller unmarked minimum. The constant difference between column 2 and column 3 arises from the measurement procedure: In this work we use peak maxima and in Reference 17, the minima of differential peaks is used. Thus, this shift is not unexpected and a one-to-one correspondence is found between the members of column 2 and those of column 3.

The strongest features, B, C, and F are associated with a hole in the L_3 ($2p_{3/2}$) level: $L_3M_{4,5}M_{4,5}$,L_3,$M_{2,3}M_{4,5}$ and $L_3M_{2,3}M_{2,3}$ respectively[18]. These are intense but broad transitions. The $L_3M_{4,5}M_{4,5}$ (KE = 692eV), the $L_3M_{2,3}M_{4,5}$ (KE = 642eV, 637eV) and the $L_3M_{2,3}M_{2,3}$ (KE = 592eV, 587eV) are all intra-shell interactions. The observed splitting in C and F, which were smeared out in the lower resolution Auger handbook spectra, is well understood[18]. The other feature which first appears at the L_3 threshold is a weaker peak at KE = 602eV (E in Table 1). This appears to be a $L_3M_1M_{4,5}$ transition. Also, when the L_2 threshold is reached, an additional transition will contribute intensity at this energy, as will be described next.

The L_2MM transitions become accessible at hν = 720eV but in general are far less intense than their L_3MM counterparts, as discussed in Reference 1. This is due in part to the Coster-Kronig[19] decay channel, $L_2L_3M_{4,5}$, which rapidly transfers the hole into the L_3 states and thus decreases

the L_2MM intensities while maintaining the L_3MM intensities. A fairly strong $L_2M_{4,5}M_{4,5}$ peak can be observed at KE = 702eV (peak A in Table 1). The other two possibilities, $L_2M_{2,3}M_{4,5}$ and $L_2M_{2,3}M_{2,3}$ are difficult to observe, and the $L_2M_{2,3}M_{2,3}$ may overlap with the $L_3M_1M_{4,5}$ at KE = 602eV. The final feature, D in Table 1 at KE = 612eV, appears to be the $L_2M_1M_{4,5}$ peak and is fairly weak, although this is the strongest of the L_2MM features relative to its L_3MM counterpart. For the sake of argument, the results of a frozen shell model are shown in Table 1. Obviously, this model is deficient and only energy differences make any sense quantitatively, e.g., $L_2M_1M_{4,5}$ versus $L_3M_1M_{4,5}$ and $L_2M_{2,3}M_{2,3}$ versus $L_3M_{2,3}M_{2,3}$. Nevertheless, it is clear that these assignments are quite reasonable.

Moreover, the spectra shown here in Figures 2 and 3 are only a part of the overall data set. A much finer grid of spectra, taken with $\Delta h\nu$ = 2eV, were also collected and were used in this analysis, although space limitation precludes their inclusion here.

Finally, one last observation should be made. Because x-ray absorption at the L_2 and L_3 edges is such a crucial part of the resonant photoemission process and because very strong absorption circular dichroism has been observed for both monolayers[3] and multilayers[4], it was plausible that a magnetic circular dichroism effect might be seen in resonant photoemission. Unfortunately, no such effects were observed.

CONCLUSIONS

An extensive resonant photoemission investigation of 4 ML Fe/Cu(001) and bulk Fe were performed. All observed resonance features can be explained by assignment as Auger peaks, so the increased intensity of the high binding energy 3s multiplet feature at resonance appears to be related to the overlap with the $L_3M_1M_{4,5}$ (or $L_2M_1M_{4,5}$) Auger transition and does not uniquely establish this feature as arising from d-mixing. This seriously calls into question the arguments

proposed earlier in Reference 1, where the variation in spectral intensities of the components of the 3s doublet were used to support a configuration-based model of photoelectron emission. The apparent variation of the 3s doublet components appears to be due merely to the onset of an Auger transition at the L3 threshold.

ACKNOWLEDGMENTS

Work performed under the auspices of the U.S. Department of Energy by the Lawrence Livermore National Laboratory under contract number W–7405–ENG-48. These measurements were made on Beamline 8–2 at the Stanford Synchrotron Radiation Laboratory. Beamline 8–2 is part of the UC/National Laboratories Participating Research Team (PRT) facilities. The authors with to thank Ms. Karen Clark for clerical support of this work.

REFERENCES

1. G. Van Der Laan, B.T. Thole, H. Ogasawara, Y.S. Seino, and A. Kotani, Phys. Rev. B 46, 7221 (1992); G. Van Der Laan, M. Surman, H.A. Hoyland, C.F.J. Flipse, B.T. Thole, Y. Seino, H. Ogasawara, and A. Kotani, Phys. Rev. B 46, 9336 (1992).

2. G.D. Waddill, J.G. Tobin, and D.P. Pappas, Phys. Rev. B 46, 552 (1992).

3. J.G. Tobin, G.D. Waddill, and D.P. Pappas, Phys. Rev. Lett. 68, 3642 (1992).

4. A.F. Jankowski, G.D. Waddill, and J.G. Tobin, Symp. Proc. Mater. Res. Soc. 313 (1993); G.D. Waddill, J.G. Tobin, and A.F. Jankowski, J. Appl. Phys. (1993), accepted.

5. C. Carbone, T. Kackel, R. Rochow, and W. Gudat, Z. Phys. B 79, 325 (1990).

6. F.U. Hillebrect, R. Jungblut, and E. Kisker, Phys. Rev. Lett. 65, 2450 (1990).

7. D.P. Pappas, G.D. Waddill, and J.G. Tobin, J. Appl. Phys. 73, 5936 (1993). The derivation of parallel and anti-parallel shown in Figure 3 of Reference 7 was inconsistent and has been reversed in this work.

8. C. Carbone and E. Kisker, Solid State Commun. 64, 1107 (1988); F.U. Hillebrecht, C.H. Roth, R. Jungblut, E. Kisker, and A. Bringer, Europhys. Lett. 19, 711 (1992); R. Jungblut, C.J. Roth, F.U. Hillebrecht, and E. Kisker, Surf. Sci. 269/270, 615 (1992).

9. B. Sinkovic, P.D. Johnson, N.B. Brookes, A. Clarke, and N.V. Smith, Phys. Rev. Lett. 65, 1647 (1990).

10. C.H. Roth, F.U. Hillebrecht, H.B. Rose, and E. Kisker, Phys. Rev. Lett. 70, 3479 (1993).

11. A. Kotani and Y. Toyozawa, "Theoretical Aspects of Inner Level Spectroscopy," in "Synchrotron Radiation," ed. C. Kunz, Springer Verlag, Berlin, (1979).

12. K.G. Tirsell and V.P. Karpenko, Nucl. Inst. Meth. A291, 511 (1990).

13. L.J. Terminello, G.D. Waddill, and J.G. Tobin, Nucl. Instrum. Meth. A319, 271 (1992).

14. Z. Hussain, private communication.

15. J.G. Tobin, G.D. Waddill, Hua Li, and S.Y. Tong, Symp. Proc. Mater. Res. Soc. 295, 213 (1993).

16. "X-Ray Data Booklet," J. Kirz, et. al., ed, LBL, 1986.

17. "Handbook of Auger Electron Spectroscopy," Physical Electronics, Eden Prairie, MN.

18. "Practical Surface Analysis by Auger and X-ray Photoelectron Spectroscopy", ed. D. Briggs and M.P. Seah, John Wiley & Sons, NY, 1983.

19. "Photoemission in Solids I," ed. M. Cardona and L. Ley, Springer Verlag, Berlin, 1978; L.C. Feldman and J.W. Meyer, "Fundamentals of Surface and Thin Film Analysis," North Holland, NY, 1986.

FIGURE CAPTIONS

Figure 1: Magnetic x-ray circular dichroism in photoemission of the fcc-Fe 3p core level. The bottom panel shows the alignment of the Fermi edge, which allows for a direct comparison of the 3p binding energies in the top panel. The sample was 2 ML Fe/Cu(001), with perpendicular magnetization. Taken from Reference 7, the circularly polarized x-rays were incident along the sample normal and the electron emission direction was at 55° from normal, approximately in the [210] plane.

Figure 2: Wide photoelectron emission scans of 4ML of Fe/Cu(001) at a series of photon energies near the $2p_{3/2}$ (707eV) and $2p_{1/2}$ (720eV) thresholds. All scans shown were taken with linear polarization, with the photons incident at 45° from the sample normal. The electrons were collected at an angle of 45° from the surface normal, with the electron momentum parallel to the photon electric polarization vector.

Figure 3: Similar to Figure 2, but here the sample is a bulk-like Fe film (25ML) on Cu(001). Note the absence of Cu spectral features. All scans shown were taken with linear polarization, at normal incidence and the electrons were collected at an angle of 45° from the normal.

Figure 4: Diagrams of direct and resonance channels in core-level photoemission. Here, emission from the 3p level is illustrated, with the $2p_{3/2}$ ionization providing the auxiliary channels.

Table 1

Constant	B^F	Constant	KE	Auger Features$^{\Delta}$	Frozen Shell Model	
	B^F(eV)$^{\neq}$		KE(eV)	KE(eV)	$KE = B^F_1 - B^F_2 - B^F_3 - \Phi$	
VB($M_{4,5}$)	~2	A	702	716	$L_2M_{4,5}M_{4,5}$	712eV
Fe3p($M_{2,3}$)	53	B*	692	703*	$L_3M_{4,5}M_{4,5}$	699eV
Cu3p	75,77	C*	642,637	651*	$L_3M_{2,3}M_{4,5}$	648eV
Fe3s(M_1)	92	D	612	(~620)	$L_2M_1M_{4,5}$	623eV
Cu3s	120	E	602	610	$L_3M_1M_{4,5}$	610eV
					$L_2M_{2,3}M_{2,3}$	610eV
		F*	592,587	598*	$L_3M_{2,3}M_{2,3}$	597eV

* = Strong Feature

Δ = From Reference 17

$^{\neq}$ = From Reference 16

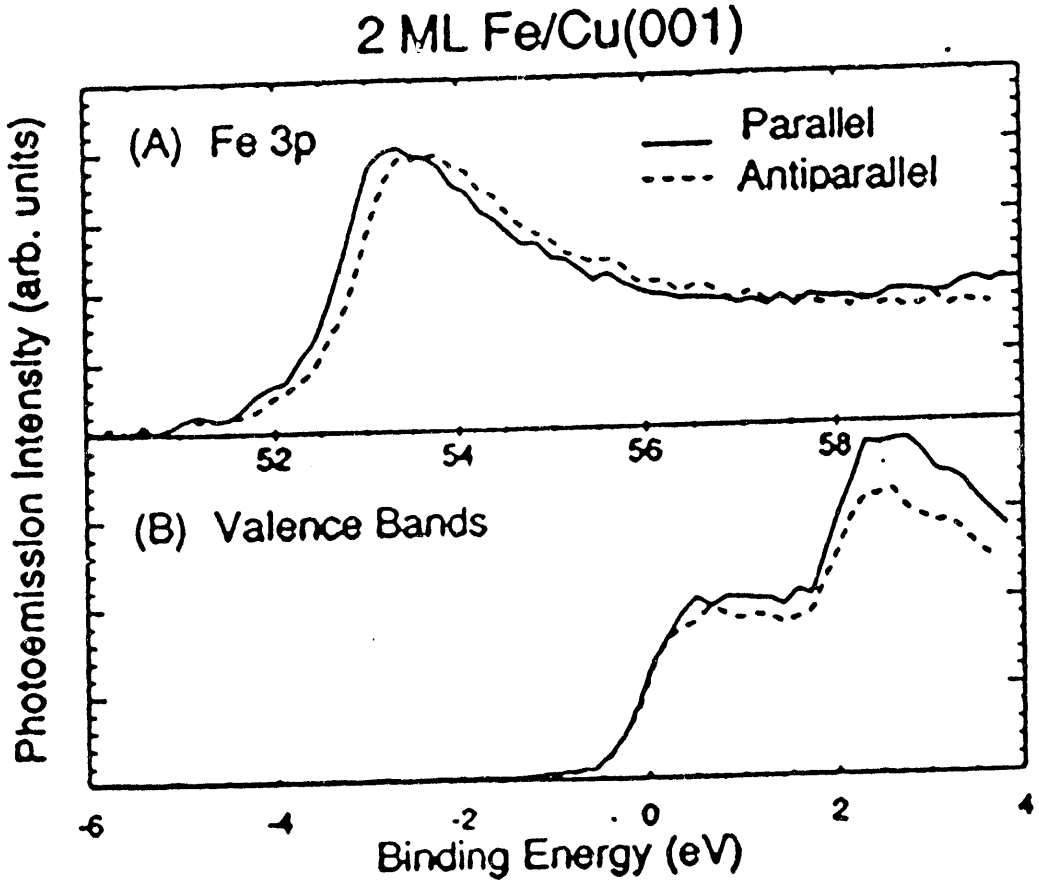
2 ML Fe/Cu(001)
(A) Fe 3p
Parallel
Antiparallel
52
54
56
58
(B) Valence Bands
Photoemission Intensity (arb. units)
-6
-4
-2
0
2
4
Binding Energy (eV)

FIGURE ONE

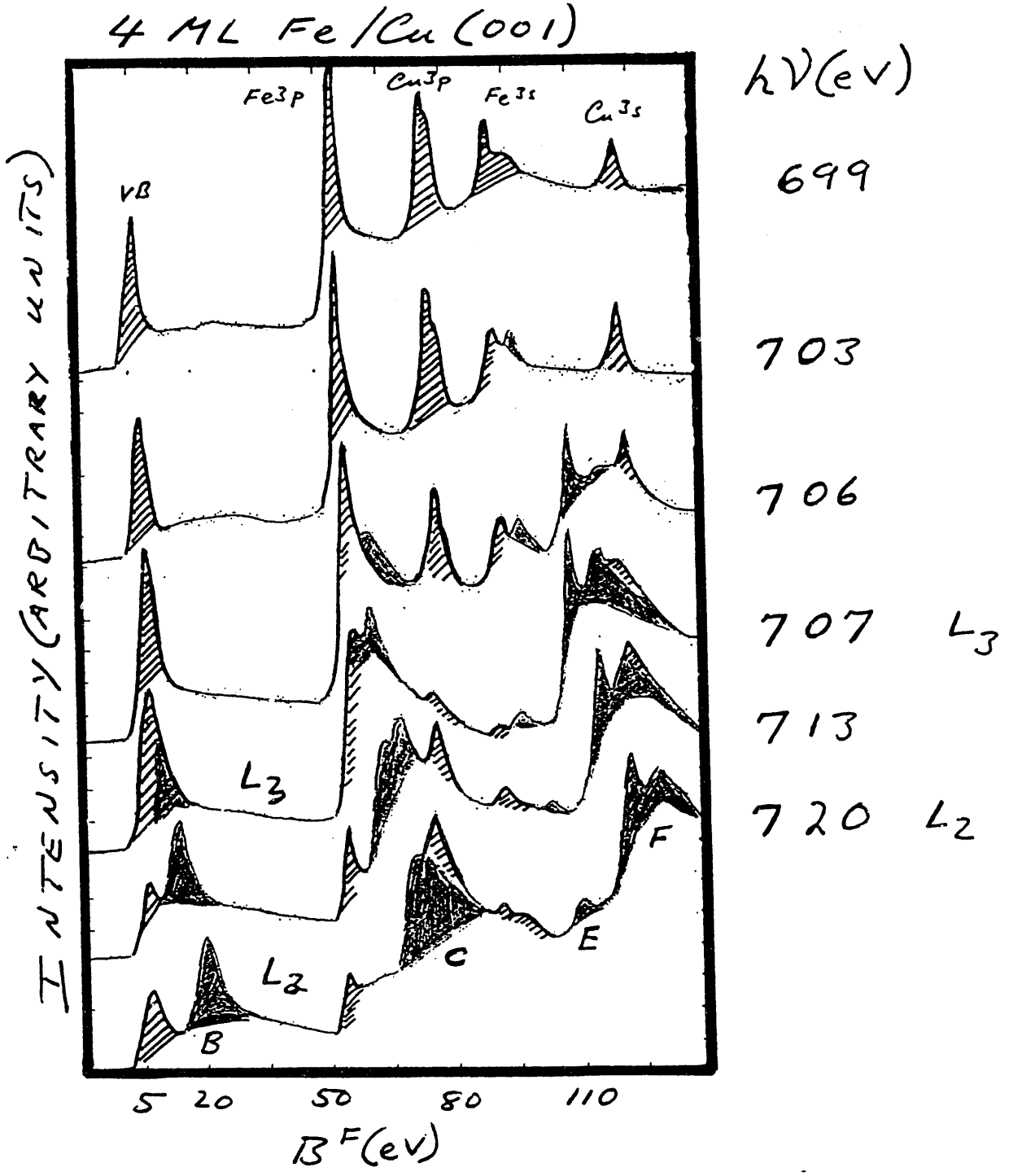
4 ML Fe/Cu(001)
hν(eV)
INTENSITY (ARBITRARY UNITS)
Fe3P
Cu3P
Fe3s
Cu3s
VB
699
703
706
707
L3
713
720
L2
L3
L2
B
C
E
F
5
20
50
80
110
B^F(eV)

FIGURE 2

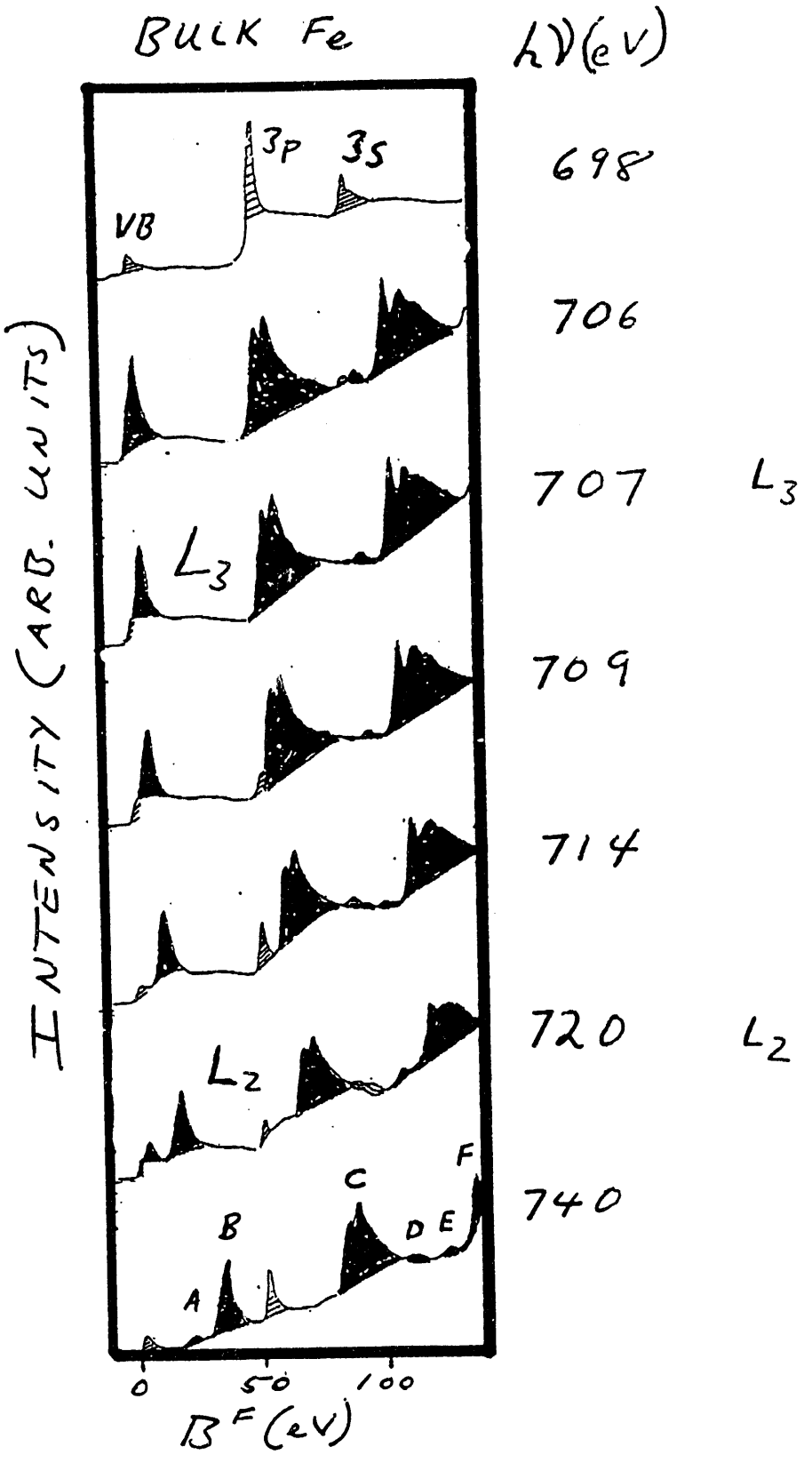
BULK Fe
hν(eV)
3P
3S
VB
698
706
707
L3
709
714
720
L2
740
A
B
C
D
E
F
INTENSITY (ARB. UNITS)
0
50
100
BF (eV)

FIGURE 3

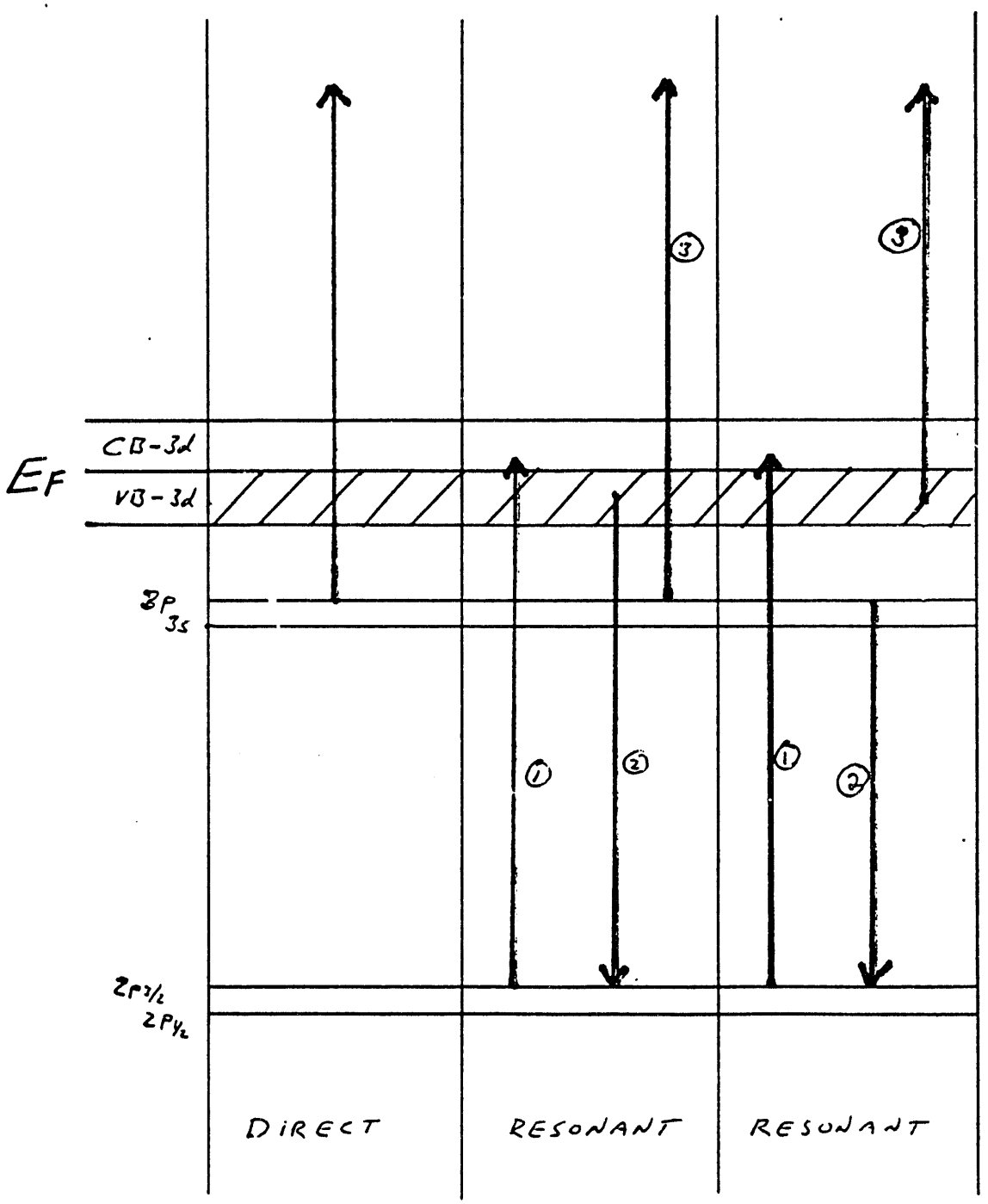
CB-3d
E_F
VB-3d
$2P_{3s}$
$2P_{1/2}$
$2P_{1/2}$
$2P_{1/2}$
1
2
3
DIRECT
RESONANT
RESONANT

FIGURE 4

DATE
FILMED
4/11/94
END